

Characteristic Structure and Environment in FAD Cofactor of (6–4) Photolyase along Function Revealed by Resonance Raman Spectroscopy

Jiang Li,^{†,‡} Takeshi Uchida,^{†,‡,||} Takehiro Ohta,^{†,⊥} Takeshi Todo,[§] and Teizo Kitagawa^{*,†,‡,∇}

Okazaki Institute for Integrative Bioscience, National Institutes of Natural Sciences, Myodaiji, Okazaki, Aichi 444-8787, Japan, Department of Photoscience, School of Advanced Sciences, Graduate University for Advanced Studies, Shonan Village, Hayama, Kanagawa, 240-0193, Japan, and Radiation Biology Center, Kyoto University, Yoshidakonoe-cho, Sakyo-ku, Kyoto, 606-8501, Japan

Received: May 16, 2006

A pyrimidine–pyrimidone (6–4) photoproduct and a cyclobutane pyrimidine dimer (CPD) are major DNA lesions induced by ultraviolet irradiation, and (6–4) photolyase, an enzyme with flavin adenine dinucleotide (FAD) as a cofactor, repairs the former specifically by light illumination. We investigated resonance Raman spectra of (6–4) photolyase from *Arabidopsis thaliana* having neutral semiquinoid and oxidized forms of FAD, which were selectively intensity enhanced by excitations at 568.2 and 488.0 nm, respectively. DFT calculations were carried out for the first time on the neutral semiquinone. The marker band of a neutral semiquinone at 1606 cm^{−1} in H₂O, whose frequency is the lowest among various flavoenzymes, apparently splits into two comparable bands at 1594 and 1608 cm^{−1} in D₂O, and similarly, that at 1522 cm^{−1} in H₂O does into three bands at 1456, 1508, and 1536 cm^{−1} in D₂O. This D₂O effect was recognized only after being oxidized once and photoreduced to form a semiquinone again, but not by simple H/D exchange of solvent. Some Raman bands of the oxidized form were observed at significantly low frequencies (1621, 1576 cm^{−1}) and with band splittings (1508/1493, 1346/1320 cm^{−1}). These Raman spectral characteristics indicate strong H-bonding interactions (at N5–H, N1), a fairly hydrophobic environment, and an electron-lacking feature in benzene ring of the FAD cofactor, which seems to specifically control the reactivity of (6–4) photolyase.

Introduction

Ultraviolet (UV) light irradiation to organisms causes damages of cellular DNA by forming a dimer between adjacent pyrimidine bases, which can result in mutation, cell death, and cancer afterward.¹ Most of the damaged DNA is cyclobutane pyrimidine dimer (CPD) and (6–4) photoproduct, which are repaired by CPD photolyase and (6–4) photolyase, respectively, under illumination by near-UV/visible light.^{2,3}

For CPD photolyase, structure and mechanism of the enzymatic reaction have been extensively studied. The resting CPD photolyase contains an anionic fully reduced FAD (FADH[−]) as an essential cofactor and also either 5,10-methenyltetrahydrofolate polyglutamate (MTHF) or flavin derivative as a light-harvesting chromophore.⁴ Crystal structures of CPD photolyase have demonstrated that the FAD cofactor, which is located in a deeply buried pocket within a protein matrix and held by the conserved residues through direct contacts, adopts an unusual and unique U-shaped conformation of isoalloxazine with an adenine ring in close proximity.^{5–8} The latest crystal structure of CPD photolyase complexed with a CPD-like DNA lesion shows that the adenine ring of FAD bridges the electron-donating isoalloxazine ring and the electron-

accepting substrate.⁸ The proposed repair mechanism of CPD photolyase is as follows: after recognizing and binding to CPD, the light-harvesting chromophore or FADH[−] absorbs a photon, and then, its excited state, FADH^{−*}, is formed either directly or by energy transfer from a light-harvesting chromophore. Next, FADH^{−*} transfers an electron to the CPD, which splits it into two pyrimidine monomers, and then, FADH^{−*} is converted into a neutral semiquinoid form (FADH[•]). Finally, an electron is transferred back from the repaired DNA to FADH[•] to restore the FADH[−].⁴ Transient absorption studies, however, argued against the last stage of the mechanism that the FAD remains in the semiquinoid state after repair and may be reduced to FADH[−] by a different chemical source.⁹

Since the amino acid sequence of (6–4) photolyase, especially in the FAD binding domain, is similar to that of CPD photolyase, it has been proposed that these two enzymes share a similar structure and reaction scheme.^{10–14} However, no crystal structure has been available for (6–4) photolyase, and therefore, its reaction mechanism is not well understood.¹⁵ It has been noted that (6–4) photolyase has a significantly lower quantum yield (0.05–0.1) of DNA repair compared with that of the CPD enzyme (0.7–0.98),⁴ and the reason for this remains to be explained.

For a flavin to perform a specific enzymatic reaction, control of its redox potential by a protein is indispensable.¹⁶ To explore the structure of the FAD cofactor and its environment in (6–4) photolyase, we measured resonance Raman spectra of the FAD cofactor in both the neutral semiquinoid and oxidized forms, since resonance Raman spectroscopy is a sensitive tool to probe the structure of flavin and its interactions with the protein environment.^{17,18} Normal mode assignments of Raman bands

* Corresponding author. Tel.: +81-564-59-5225. Fax: +81-564-59-5229. Email: teizo@ims.ac.jp.

[†] Okazaki Institute for Integrative Bioscience.

[‡] Graduate University for Advanced Studies.

^{||} Kyoto University.

[⊥] Present address: Division of Chemistry, Graduate School of Science, Hokkaido University, Sapporo, 060-0810, Japan.

[§] Present address: Department of Chemistry, Stanford University, 333 Campus Drive, Stanford, California 94305-5080.

[∇] Present address: Toyota Physical & Chemical Research Institute, Nagakute, Aichi, 480-1192, Japan.

for the neutral semiquinoid flavin were performed for the first time using density functional theory (DFT) calculations on lumiflavin at the B3LYP/6-31G(d) level. Our results suggest that the FAD of (6–4) photolyase has a structure in which electron density is lacking in the benzene ring and strong hydrogen bonds are formed at N5–H and N1 in an overall hydrophobic environment, and its relationship to functions will be discussed.

Experimental Methods

Enzyme Preparation. The gene of (6–4) photolyase from *Arabidopsis thaliana*¹⁹ was inserted at the *NdeI/SacI* sites of the pET-28a expression vector (Novagen). *Escherichia coli* BL21(DE3) transformed with the vector was inoculated into 0.5 L of culture in a 3-L flask and grown at 37 °C in LB medium to OD₆₀₀ of 1.5 and then cooled to 26 °C. IPTG was added to 0.2 mM. The culture was further incubated for about 24 h and then harvested. After harvest, the pellet was frozen at –80 °C, thawed, and resuspended in a lysis buffer (20 mM sodium phosphate, 0.5 M NaCl, 1 mM DTT, 5% glycerol, pH 7.4). Following the sonication, the cell debris was removed by ultracentrifugation. The cell-free extract was loaded onto a HisTrap HP column (Amersham), and the fusion protein was eluted with the elution buffer (20 mM sodium phosphate, 0.5 M NaCl, 0.5 M imidazole, pH 7.4). Then, the sample was applied to a HiTrap Heparin HP column (Amersham) and eluted with a linear gradient of NaCl from 0.3 to 1 M. The sample was identified as a monomeric form by a HiLoad 16/60 Superdex 200 prep grade column (Amersham). Starting from 2 L of the *E. coli* culture, ca. 12 mg of the purified protein was obtained after the Heparin column.

The purified enzyme was stored in 20 mM sodium phosphate (pH 7.4) containing 0.5 M NaCl. Purity of the protein after the Heparin column was determined by SDS–PAGE, and the molecular weight of the monomeric enzyme was confirmed with the gel filtration method under the assumption that the elution volume of the Superdex 200 column was the same as that scaled by Gel Filtration Calibration Kit (Amersham). The concentration of the oxidized form of the enzyme was estimated on the basis of the FAD absorbance at 450 nm ($\epsilon_{450} = 1.12 \times 10^4 \text{ M}^{-1} \text{ cm}^{-1}$),²⁰ and that of the neutral semiquinoid form was estimated from the absorbance at 580 nm ($\epsilon_{580} = 4.8 \times 10^3 \text{ M}^{-1} \text{ cm}^{-1}$).²¹

Enzyme Photoreduction. (6–4) Photolyase as purified is composed of semiquinoid FAD and oxidized FAD. All the semiquinoid enzymes in this mixture were completely oxidized by air in 48 h because of its sensitivity to oxygen. To prepare the semiquinoid form, the oxidized enzyme was photoreduced by laser irradiation at 442 nm from a He–Cd laser (Kimmon Electric, IK4101R–F). First, 100 μL of the solution containing 150 μM (6–4) photolyase was placed in a cylindrical Raman cell and sealed with a rubber septum. Then, the inside of the cell was replaced with N₂, and the cell was spun at a rate of 2000 rpm. The laser light was focused onto the sample evenly with a quartz lens of 150-mm focal length to increase the efficiency of photoreduction. To avoid the cell heating by laser illumination, the spinning cell was cooled by flushing with cold N₂ gas passed through liquid N₂. About 30 min illumination with 30 mW laser light was sufficient to reduce 150 μM (6–4) photolyase. Reduction of a majority of the oxidized FAD to the semiquinoid form was confirmed with absorption spectra.

Enzyme Activity. The method for measuring the enzyme activity of (6–4) photolyase was based on the procedure established for CPD photolyase.²² A substrate of the damaged DNA was prepared through irradiation of p(dT)₈ by 254 nm

UV light from a UV transilluminator (Vilber Lourmat, TFX-20-MC) with 6.4 mW/cm² of intensity for 30 min using the cylindrical spinning cell cooled by cold N₂. The complex of 2 μM (6–4) photolyase with 50 μM damaged p(dT)₈ in 50 mM Tris–HCl (pH 7.4), 200 mM NaCl, and 1 mM DTT was illuminated by tungsten light (Sigma Koki, PHL-150) at room temperature. The UV–vis absorption spectrum of the reacting sample in the spinning cell was measured at 1-min intervals.

Absorption and Resonance Raman Spectroscopy. Optical absorption spectra of samples were recorded with a Hitachi UV-3310 UV–vis spectrophotometer at room temperature. Resonance Raman spectra were obtained with a single monochromator (Jobin Yvon, SPEX750M) equipped with a liquid N₂-cooled CCD detector (Roper Scientific, Spec10:400B/LN). The excitation wavelengths used were 568.2 and 488.0 nm from a krypton–argon mixed gas ion laser (Spectra Physics, BeamLok 2060) for the semiquinoid and oxidized forms, respectively. The laser power at the sample point was 5 mW. Rayleigh scattering was removed with appropriate holographic notch filters (Kaiser Optical Systems). Raman shifts were calibrated with indene, and the accuracy of the peak positions of the well-defined Raman bands was $\pm 1 \text{ cm}^{-1}$.

An aliquot of the 150 μM enzyme solution in 20 mM sodium phosphate buffer at pH 7.4 containing 0.5 M NaCl was used for the measurement of the semiquinoid form, while the 80 μM enzyme or isolated FAD solution in the same buffer was used for the measurements of the oxidized enzyme or isolated FAD. All the measurements were performed with a spinning Raman cell containing 100 μL of the sample solution, and the semiquinoid samples were purged with N₂ to avoid the oxidation. All samples were cooled with cold N₂ gas. The structureless background in the final spectrum was removed by a polynomial subtraction procedure by *Igor Pro 5.03* (Wave-Metrics).

Density Functional Theory Calculations. To analyze the Raman bands of the FAD neutral semiquinoid form, geometry optimizations and frequency calculations were carried out for a model compound, lumiflavin, in its neutral radical semiquinoid form by the DFT method on the B3LYP/6-31G(d) level. To see the deuterated effect of flavin on calculated normal modes and those frequencies, the H atom bound at the N3 and N5 positions was replaced with the D atom. The structures with the minimal energy were confirmed by the absence of imaginary frequencies. The obtained frequencies were scaled by the widely accepted single scaling factor of 0.9614.²³ All calculations were carried out on an SGI2800 high-performance computer (Research Center for Computational Science, Okazaki) using the program package *Gaussian 03*.²⁴

Results

Enzyme Activity of (6–4) Photolyase. Figure 1 shows the time course of dimer repair observed with 2 μM (6–4) photolyase and 50 μM damaged p(dT)₈ in the reaction buffer as described in the Experimental Methods. For the damaged DNA, the 266 nm band of normal DNA is decreased significantly, and a band at 325 nm of the (6–4) photoproducts²⁵ is appreciable. Along the illumination of white light for the damaged DNA in the presence of (6–4) photolyase, reappearance of the band at 266 nm (a) and disappearance of the band at 325 nm (b) were observed, while no change was observed in the absence of the enzyme (data not shown), demonstrating that the His-tagged enzyme used in this study is active like a GST-tagged enzyme.¹⁹

Absorption Spectra of (6–4) Photolyase. The three redox states including oxidized (FAD_{ox}), semiquinoid (FADH[•]), and

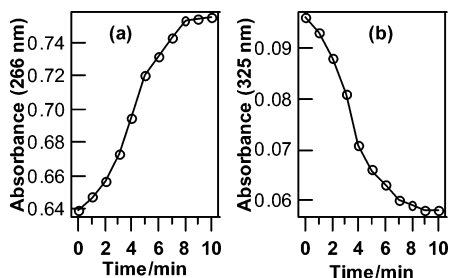


Figure 1. Effect of illumination time on the extent of dimer repair by the His-tagged enzyme used in this experiment observed with damaged p(dT)₈. Absorbance at 266 nm (a) and that at 325 nm (b) of (6–4) photoproducts are plotted against time.

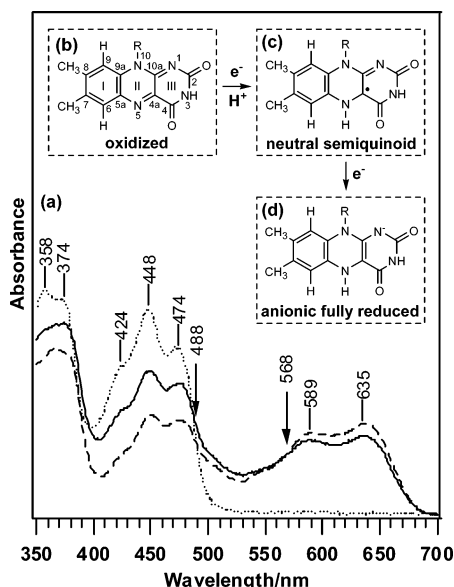


Figure 2. Absorption spectra of (6–4) photolyase from *Arabidopsis thaliana* (a) and the structure and atomic numbering schemes of flavin in three redox states (b–d). For (a), the solid line shows the spectrum of the enzyme immediately after purification, which is a mixture of a neutral semiquinoid form and an oxidized form, the dashed line shows the photoreduced enzyme with a majority amount of the neutral semiquinoid form, and the dotted line shows that of the fully oxidized form. The arrows indicate the Raman excitation wavelengths. (b) Oxidized form. (c) Neutral semiquinoid form. (d) Anionic fully reduced form.

fully reduced (FADH^-) forms, are possible for an isoalloxazine ring, and their structures and atomic numbering are illustrated in Figure 2(b–d). Immediately after purification, the enzyme was a mixture of FAD_{ox} and FADH^\bullet as shown by a solid line in Figure 2a. The fully oxidized form, which is shown by a dotted line in Figure 2a, was obtained by exposure of the above mixture to air for 48 h. The absorption spectrum of the fully oxidized (6–4) photolyase is remarkably different from that of FAD in a polar solvent, while it is similar to that in a nonpolar solvent.²⁶ The similarity of absorption spectra suggests that FAD in (6–4) photolyase is bound in a less polar environment.

The semiquinoid form was obtained by reduction of the oxidized enzyme by irradiation of blue light as explained in the Experimental Methods, which gave an absorption spectrum as the dashed line in Figure 2a. The absorption maxima at 589 and 635 nm of a solid and dashed line in Figure 2a are due to the π – π^* electronic transition of FADH^\bullet , while they are completely absent in the spectra of FAD_{ox} and FADH^- (data not shown). On account of these absorption spectra, 568.2 nm was chosen as the Raman excitation wavelength to selectively

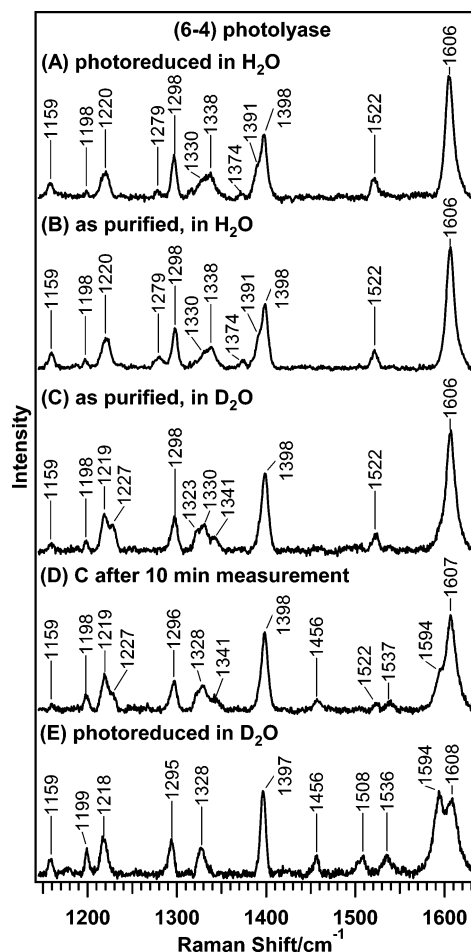


Figure 3. Resonance Raman spectra of (6–4) photolyase from *Arabidopsis thaliana* which was photoreduced by blue light in H₂O (A), immediately after purification in H₂O (B) and in D₂O (C). Spectrum (D) was observed after 10 min in the repeated measurement in D₂O. Spectrum (E) were observed for the enzyme which was oxidized completely first and photoreduced subsequently by blue light in D₂O. The Raman excitation wavelength was 568.2 nm.

enhance the neutral semiquinoid form, while 488.0 nm was chosen to enhance the pure oxidized form.

Resonance Raman Spectra of Semiquinoid (6–4) Photolyase. The resonance Raman spectra of the photoreduced form in H₂O is shown in Figure 3A. The prominent bands in the H₂O solution at 1606, 1522, 1398, 1298, and 1220 cm⁻¹ correspond well to bands of riboflavin neutral semiquinoid radical generated by pulse radiolysis at 1617, 1542, 1387, 1296, and 1225 cm⁻¹, which are Raman spectroscopically distinct from those of anion and cation radicals.²⁷ Therefore, Figure 3A demonstrates the formation of a neutral semiquinone (Figure 2c) in (6–4) photolyase. The spectrum B in Figure 3 is of the enzyme immediately after purification. Although the enzyme contains some amount of the oxidized form as shown in Figure 2a, the observed Raman spectrum (Figure 3B) is almost identical to that of the photoreduced form (Figure 3A), since the bands are solely ascribed to the semiquinoid form due to the advantage of resonance effect of Raman excitation at 568.2 nm.

Spectrum C was observed for the sample whose solvent was replaced with D₂O immediately after purification of the enzyme in H₂O. Spectrum C is different from spectrum B with regard to the bands at 1341, 1323, and 1227 cm⁻¹, indicating that deuteration occurred. However, prolonged measurements brought about further changes. After 10 min of measurements, for example, the bands at 1522 and 1606 cm⁻¹ seemed to split into

TABLE 1: Raman Frequencies (cm^{-1}) of Neutral Radical Semiquinoid Flavins and Flavoproteinsⁱ

compound	solvent	Raman bands											
^a (6–4) PL, FADH ^o	H ₂ O	1606		1522		1398	1374	1338	1330	1298	1279	1220	1198
^a (6–4) PL, FADH ^o	D ₂ O	1608	1594	1536	1508	1456	1397		1328	1295		1218	1199
^b CPD PL, FADH ^o	H ₂ O	1607		1529			1392	1378	1347	1332	1303	1260	1222
^b CPD PL, FADH ^o	D ₂ O	1607	1593	1529	1508		1392	1378		1332	1325	1302	1260
^c CPD PL, FADH ^o	H ₂ O	1606		1528			1391			1332		1301	1220
^c CPD PL, FADH ^o	D ₂ O	1606	1594	1528			1390	1377		1332	1322	1300	1219
^d P-450 Rd, FADH ^o	H ₂ O	1611		1540			1378			1305	1264	1226	
^d P-450 Rd, FMNH ^o	H ₂ O	1611		1532			1388			1304	1268	1227	1200
^e Ad Rd, FADH ^o	H ₂ O	1611						1344		1310	1271		
^f Fd, FMNH ^o	H ₂ O	1611		1535			1391	1378	1333	1314	1308	1269	1232
^g Fd, FMNH ^o	D ₂ O	1611					1386						
^h riboflavin, RFH ^o	H ₂ O	1617		1542			1387			1296		1225	

^a This work. ^b Ref 29. ^c Ref 28. ^d Ref 32. ^e Ref 31. ^f Refs 32, 48. ^g Ref 48. ^h Ref 27. ⁱ PL: photolyase. Rd: reductase. Ad: adrenodoxin. Fd: flavodoxin. RF: riboflavin.

three and two bands, respectively, as illustrated in spectrum D. The sample of E was obtained separately by photoreduction in D₂O after complete oxidation of the purified enzyme in air. Because the proton attached at N5 of the semiquinoid flavin is released from the nitrogen atom in the oxidized form (Figure 2b), the above processes of oxidation and subsequent photoreduction in D₂O lead complete replacement of the H atom at N5 with the D atom. Accordingly, the spectral change in spectrum D compared with spectrum C seems to reflect the progress of N5-deuteration of FAD through photoreduction by the probe light along measuring time. Since spectrum C is different from either spectrum B in H₂O or spectrum E of the fully N5–D form, it is considered to reflect the N3–D form. It means that spectra C and E correspond to the N3–D/N5–H and N3–D/N5–D forms of isoalloxazine, respectively. Accordingly, the bands at 1594, 1536, 1508, and 1456 cm^{-1} are characteristic of N5–D, while those around 1200–1350 cm^{-1} are mainly due to N3–D.

Raman bands of the FADH^o of (6–4) photolyase are listed in Table 1 and are compared with those of other flavins and flavoproteins in a neutral radical form.^{27–29,31,32,48} It is noted that the frequencies of prominent Raman bands of (6–4) photolyase are close to those of CPD photolyase. No Raman bands have been found so far in the 1400–1500 cm^{-1} region for the neutral semiquinoid flavins.²⁷ For (6–4) photolyase in the N5–D form, however, a band was observed at 1456 cm^{-1} for the first time. The reported Raman studies on CPD photolyase have not discussed the bands in this region because of the interference by the bands of Hepes²⁹ or glycerol²⁸ in the solvent. We can avoid this problem by using 20 mM phosphate buffer without glycerol. Vibrational assignment of these bands will be described quantitatively later on the basis of DFT calculations.

Resonance Raman Spectra of Oxidized (6–4) Photolyase.

Figure 4 shows the resonance Raman spectra of the oxidized (6–4) photolyase in H₂O (A) and D₂O (B). The vibrational assignment of the oxidized flavin has been well-established,^{33–36} and the customary numbering of Raman bands is given in the upper part of the figure. Band I of the oxidized flavin, which is attributed to an almost pure ring I mode and is generally observed around 1630 cm^{-1} ,^{32,33,36–45} appeared at a distinctly lower frequency for (6–4) photolyase (1621 cm^{-1} in both H₂O and D₂O). All bands above 1340 cm^{-1} are H₂O/D₂O insensitive, meaning that they arise from rings I and/or II, since neither ring has exchangeable protons. However, the bands at 1254, 1266, and 1320 cm^{-1} in H₂O were shifted to lower or higher frequencies in D₂O (1241 and 1330 cm^{-1}). These are characteristic of the C2–N3 and N3–C4 stretching modes coupled with the N3–H bending mode, which exhibits a higher

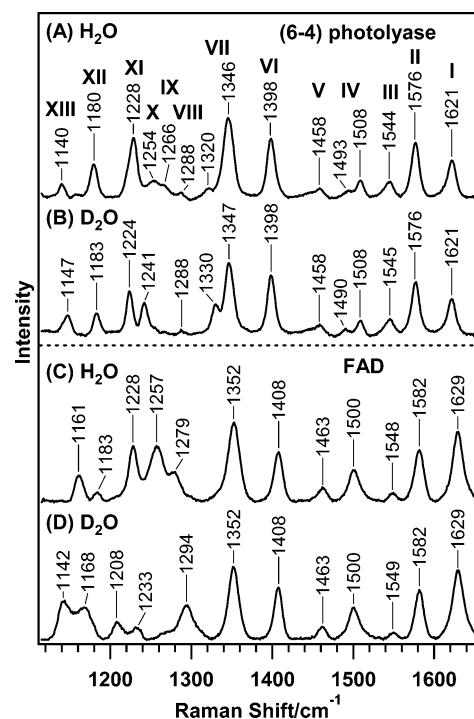


Figure 4. Resonance Raman spectra of oxidized (6–4) photolyase from *Arabidopsis thaliana* in H₂O (A) and D₂O (B) and those of free FAD in H₂O (C) and D₂O (D). The excitation wavelength was 488.0 nm. The FAD solution contains 4 M KI to quench fluorescence. Band numbering is according ref 34.

frequency shift upon removal of the coupling with N–H bending vibration in the N3–D form³⁸ but is shifted to lower by the coupling with the N3–D bending vibration.

Since the Raman spectrum of the oxidized CPD photolyase has not been reported yet, the spectra of the protein-free FAD in H₂O (C) and D₂O (D), measured under the same experimental condition except for addition of 4 M KI to quench the fluorescence, are presented for comparison in the lower part of Figure 4. The bands above 1350 cm^{-1} are generally insensitive to the H/D substitution, in agreement with the results of (6–4) photolyase. The bands of free FAD in H₂O in the 1150–1300 cm^{-1} region are shifted in D₂O in a complicated way, reflecting the participation of the N3–H bending vibration. The differences in these frequencies between (6–4) photolyase and free FAD are caused by differences in H-bonding at N3–H with the protein in water.

From the comparison of rings I and II modes between (6–4) photolyase and free FAD, it is noticed that frequencies are generally lower and the intensity of the band at 1621 cm^{-1} (band

TABLE 2: Assignments of Raman Bands of Neutral Radical Semiquinoid Flavin in (6–4) Photolyase

observed (6–4) photolyase			calculated frequencies for lumiflavin ^a				approximate descriptions
H ₂ O	D ₂ O intermediate ν/cm^{-1}	D ₂ O	mode	N3–H N5–H ν/cm^{-1}	N3–D N5–H $\Delta\nu/\text{cm}^{-1}$	N3–D N5–D $\Delta\nu/\text{cm}^{-1}$	
1606	1606	1608	ν_{75}	1602	–1	–1	ν (ring I)
		1594	ν_{74}	1591	0	–7	ν (ring I), δ (N5–H), ν (N1=C _{10a}), ν (C _{4a} –N ₅)
		1536	ν_{73}	1539	0	0	ν (ring I), ν (N1=C _{10a})
1522	1522	1508	ν_{72}	1503	0	–2	ν (ring I), δ (N5–H)
		1456	ν_{71}	1495	–1	–46	δ (N5–H), ν_{asym} (C _{4a} –N ₅ –C _{5a}), ν (N1=C _{10a})
1398	1398	1397	ν_{61}	1398	0	–2	ν (ring I), ν (N1=C _{10a}), ν (C _{4a} –N ₅), ν_{asym} (C _{9a} –N ₁₀ –C _{10a})
1338	1330	1328	ν_{59}	1345	–4	–19	δ (N5–H), δ (N3–H), ν_{sym} (C _{9a} –N ₁₀ –C _{10a}), ν_{sym} (C _{10a} –N ₁ –C ₂), ν_{asym} (N ₃ –C ₄ –C _{4a})
1330			ν_{58}	1335	–124	–170	δ (N3–H), δ (N5–H)
1298	1298	1295	ν_{57}	1312	–1	–5	ν (ring I), ν_{sym} (C _{9a} –N ₁₀ –C _{10a}), δ (N5–H)
1279			ν_{56}	1298	+5	+2	ν (ring I), ν_{asym} (C _{9a} –N ₁₀ –C _{10a}), δ (N3–H), δ (N5–H)

^a Calculated using density functional theory (DFT) by *Gaussian 03* with B3LYP/6-31G(d) basis functions.

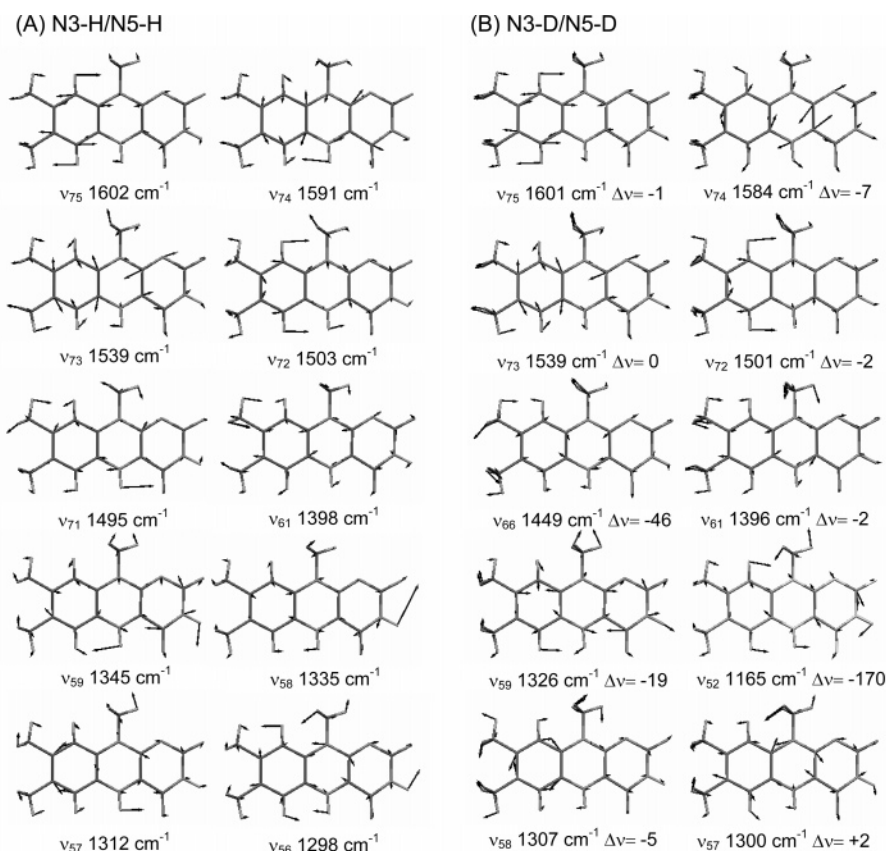


Figure 5. Normal modes of some typical marker bands for neutral radical semiquinoid lumiflavin (A) and its corresponding N3-D/N5-D form (B). Vibrational frequencies and displacements were calculated by DFT method using *Gaussian 03* with B3LYP/6-31G(d) basis functions.

I) is weaker for protein than for free FAD. Since band II is known to exhibit downshifts upon formation of a hydrogen bond at N1,³⁶ its lower frequency suggests that a strong hydrogen bond is formed at N1 of FAD in (6–4) photolyase. Splittings of band IV (1508 and 1493 cm^{-1}) and band VII (1346 and 1320 cm^{-1}) of the oxidized (6–4) photolyase are used as a marker of “buried” character of the flavin environment.³³ In fact, both bands are observed as a single band for free FAD (spectrum C), while it is split in a solid state.³³ Therefore, this observation indicates that the isoalloxazine ring of (6–4) photolyase is held in a well-formed protein pocket from which water molecules might be excluded. In addition, it is noted that the downshifted and weakened band I (1621 cm^{-1}), intensified band III (1544 cm^{-1}), downshifted band VI (1398 cm^{-1}), downshifted and weakened band IX (1266 cm^{-1}), weakened band X (1254 cm^{-1}), downshifted and intensified band XII (1180 cm^{-1}), and weak-

ened band XIII (1140 cm^{-1}) all resemble the spectral characteristics of flavin placed in a less polar solvent.^{40,46}

Density Functional Theory Calculation for Neutral Radical Semiquinoid Lumiflavin. Since there has been no theoretical treatment of vibrational spectra of neutral semiquinone of flavin, we carried out DFT calculations on lumiflavin at B3LYP/6-31G(d) level, and the results are summarized in Table 2, where the frequencies observed for (6–4) photolyase in H₂O and D₂O are compared with those calculated (scaled by a factor of 0.9614)²³ for the N3–H/N5–H, N3–D/N5–H, and N3–D/N5–D forms. In addition, included are the mode numbers and the approximate descriptions for vibrational character. Calculated vibrational modes are also illustrated in Figure 5, where the displacements of atoms are explicitly represented.⁴⁷ Cartesian coordinates of atoms in the minimal potentials obtained are given

by Table S1 in the Supporting Information. The mode numbers are assigned tentatively in the order of increasing frequency, although the numbering is not established yet. Tentative assignments of the Raman bands observed for FADH^o in (6–4) photolyase are also contained.

According to this calculation, the prominent band at 1606 cm⁻¹ in H₂O can be assigned to an overlapped band of ν_{75} and ν_{74} , which include ring I and primarily ring II vibrations, respectively. ν_{75} does not shift upon N5–H deuteration, while ν_{74} downshifts by 7 cm⁻¹ due to fairly large involvement of N5–H bending motion in the ν_{74} mode. Therefore, they are observed as separate bands in D₂O.

The alteration of resonance Raman band in the 1400–1550 cm⁻¹ region upon deuterium substitution exhibits complex behavior. The 1522 cm⁻¹ band observed in H₂O seems to split into 1536, 1508, and 1456 cm⁻¹ in D₂O, as judged from concomitant intensity decrease of the 1522 cm⁻¹ band and intensity increase of those three bands. These bands were presumably assigned to the three computed normal modes, ν_{73} , ν_{72} , and ν_{71} , in the 1500–1540 cm⁻¹ region. Upon deuteration, the normal coordinate compositions are altered for the vibrational modes in this region and thereby resonance Raman intensity redistribution, which are interpreted below. The ν_{73} mode is mainly composed of the N1=C10a stretching and ring I symmetric modes and is expected to get strong resonance Raman enhancement due to a large change in polarizability along those symmetric modes. Furthermore, appreciable excited-state distortion of the N1=C10a bond is expected upon the π – π^* excitation at 568.2 nm, and it would cause redistribution of electron density regarding the N1=C10a bond. The ν_{73} mode does not include vibration arising from N–H motion and thus does not show a large change in both the frequency and the normal mode in the deuterated form. The ν_{72} mode mainly consists of C–H bending in ring I and N–H bending which is coupled weakly with the ring I mode. Upon deuteration, the coupling of the N–H motion is removed, showing a slight downshift in the frequency. The ν_{72} mode in the H-form may not be strongly resonance enhanced due to the C–H bending character of the vibrational mode. However, upon deuteration, the ν_{72} normal mode compositions are slightly altered. As mentioned above, the coupling with N–H bending is removed, and the mixing of the N1=C10a stretching mode could cause resonance enhancement of Raman intensity. The ν_{71} mode at 1495 cm⁻¹ is mainly composed of N5–H bending, to which N1=C10a stretching and the asymmetric C4a–N5–C5a stretching [$\nu_{\text{asym}}(\text{C4a–N5–C5a})$] that can be intensity-enhanced by the π – π^* excitation are coupled. This mode should show a large deuterium isotope shift, and the corresponding mode in the deuterium substituted form could be found as the ν_{66} mode at 1449 cm⁻¹. Thus, the 1456 cm⁻¹ band observed in D₂O would arise from the ν_{66} mode. In the H₂O form, however, the ν_{66} mode is mainly composed of C–H bending motion of the methyl substituents of ring I, which would not gain resonance Raman enhancement. When N5 is deuterated, ν_{66} contains the N1=C10a and C4a–N5 stretchings and accordingly gains Raman intensity.

The intense band of Figure 3A at 1398 cm⁻¹ is assignable to ν_{61} , which involves N1=C10a and C4a–N5 stretching. Therefore, its frequency would be insensitive to deuterium exchange as observed both theoretically and experimentally. The shoulder peak at 1391 cm⁻¹ and the nearby weak band at 1374 cm⁻¹ disappear in D₂O. A couple of bands around 1338 cm⁻¹ probably arise from ν_{59} and ν_{58} . The ν_{58} mode is almost pure N3–H and N5–H deformational mode, which exhibits a large

downshift in the frequency upon deuteration. The bands of Figure 3A at 1298 and 1279 cm⁻¹ are probably assigned to ν_{57} and ν_{56} , respectively.

Discussion

Comparison with CPD Photolyase. The marker band of the neutral semiquinoid flavin³⁰ for (6–4) photolyase was observed at 1606 cm⁻¹ (Figure 3A), which is similar to that observed for CPD photolyase at 1607²⁹ or 1606²⁸ cm⁻¹ (Table 1). These frequencies are lower than those of other flavins and flavoproteins.^{27–32,48,49} However, this marker band at 1606 cm⁻¹ in (6–4) photolyase in H₂O splits into two comparable bands at 1608 and 1594 cm⁻¹ in D₂O (Figure 3E), whereas that of CPD photolyase in D₂O remains a single band with a shoulder at 1593 cm⁻¹, which is very similar to that of (6–4) photolyase obtained after prolonged measurement in Figure 3D. Figure 3D is inferred to arise from the incompletely N5-deuterated sample, because for (6–4) photolyase, the redox cycle in this study (oxidation and subsequent photoreduction in D₂O) enforced the release of the N5 proton of flavin and replaces it with deuterium in a D₂O solvent, which gives the spectrum of the completely N5-deuterated sample as observed in Figure 3E. Consequently, it is highly likely that the reported spectrum of CPD photolyase in D₂O^{28,29} reflects an incompletely N5-deuterated enzyme. The assignment from DFT calculations that ν_{74} is low-frequency shifted but ν_{75} is invariable in the N5–D form (Table 2) also supports that the deuterium exchange at N5 causes its apparent splitting.

Another H/D-sensitive band at 1522 cm⁻¹ in H₂O splits into three bands at 1456, 1508, and 1536 cm⁻¹ in D₂O. The split band at 1508 cm⁻¹ was observed for CPD photolyase in one report²⁹ but not in the other,²⁸ while the split band at 1456 cm⁻¹ has not been observed in flavoproteins before. This apparent splitting is actually a frequency separation of accidentally degenerate bands due to a low-frequency shift of ν_{72} and ν_{71} in D₂O, while the higher-frequency counterpart (ν_{73}) is less sensitive to N5 deuteration. Although the corresponding Raman band of CPD photolyase at 1528²⁸ or 1529²⁹ cm⁻¹ had no H/D effect, a similar H/D-sensitive resonance Raman band in this region was also observed for *Clostridium Mp.* Flavodoxin.⁴⁸

A prominent H/D-insensitive band was observed at 1398 cm⁻¹ (with a shoulder at 1391 cm⁻¹) and a nearby H/D-sensitive band at 1374 cm⁻¹. The corresponding bands in CPD photolyase were observed at 1392 and 1378 cm⁻¹, respectively. Schelvis et al. proposed that the band at 1378 cm⁻¹ in CPD photolyase might be a marker for the MTHF or its structural role by stabilizing the protein environment of the FAD cofactor,²⁹ because this band was not observed for the MTHF-free mutant of CPD photolyase.²⁸ Since the purified (6–4) photolyase in this study does not contain the second chromophore, the 1374 cm⁻¹ band cannot be ascribed to the MTHF moiety. Our theoretical assignment suggests that the intense band at 1398 cm⁻¹ arises from the ν_{61} mode. Since ν_{61} involves N1=C10a and ring II stretching characters, its strong resonance Raman intensity is reasonable. The weak band at 1374 cm⁻¹ probably arises from ring III of FAD in H₂O but is shifted to lower frequencies upon N3 deuteration.

H-bonding Environment of FAD in (6–4) Photolyase. The crystal structure of *E. coli* CPD photolyase revealed the H-bonding environment of FAD as illustrated in Figure 6. Hydrogen bonds are formed at N1, N3–H, C4=O, and N5–H in CPD photolyase. The 2'-OH of the ribityl chain forms a hydrogen bond with N1 probably because of the unusual U-shaped FAD structure. N3–H donates a hydrogen bond to

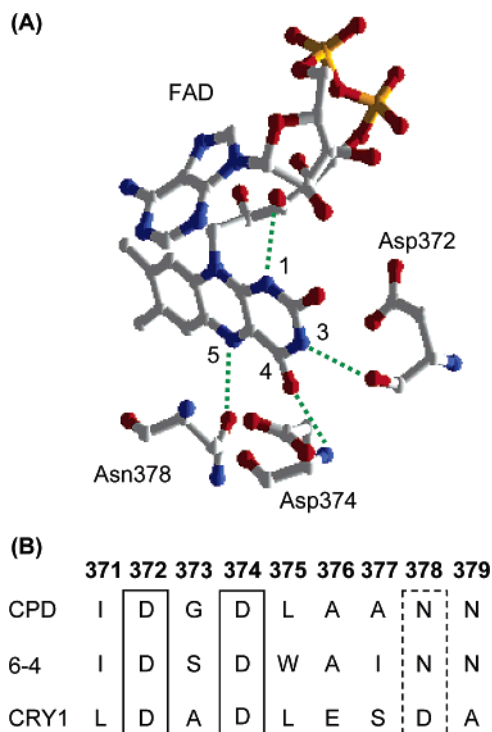


Figure 6. Structure and sequence alignment for flavin center. (A) Crystal structure of *E. coli* CPD photolyase. (B) Alignment of *E. coli* CPD photolyase, *Arabidopsis thaliana* (6-4) photolyase, and *Arabidopsis thaliana* cryptochrome 1 over the region in H-bonding distance from isoalloxazine (from refs 5, 19, 50).

Asp372 (numbering in *E. coli* CPD photolyase), C4=O accepts a hydrogen bond from Asp374, and N5-H donates a hydrogen bond to Asn378. These amino acids involving hydrogen bonds are conserved in (6-4) photolyase. A very similar U-shaped FAD and H-bonding environment were also observed for the structure of the photolyase-like domain of cryptochrome 1 from *Arabidopsis thaliana*, except that the Asn378, which is contacted with N5-H, is replaced by Asp.⁵⁰ A sequence alignment in this region is illustrated in Figure 6B. From the sequence alignment and resonance Raman spectra of (6-4) photolyase, the presence of similar hydrogen bonds at N5-H and N1 in (6-4) photolyase is indicated as discussed below.

We have already pointed out that the 1606 cm⁻¹ marker band is assignable to an overlapped band of ν_{74} and ν_{75} . Its significantly lower frequency is a common feature to photolyases: 1607 cm⁻¹ for CPD photolyase and 1606 cm⁻¹ for (6-4) photolyase. Murgida et al. attributed the origin of the unusually low frequency of this band to a stronger hydrogen bond at N5-H,²⁸ although Schelvis et al. argued against it, because its frequency is rather insensitive to H/D exchange. However, as mentioned above, deuteration in the sample of Schelvis et al. was probably incomplete, and presumably, N5-H was not replaced with deuterium. In this study, splitting of this marker band into two comparable components at 1608 and 1594 cm⁻¹ was observed for the completely deuterated FAD cofactor in Figure 3E. The normal modes of ν_{74} assigned for 1594 cm⁻¹ band involve N5-H bending deformations (Table 2, Figure 5), which will downshift upon H-bonding at N5-H as discussed by Murgida et al. before.²⁸ Therefore, the unusually low frequency of this marker band would indicate a strong hydrogen bond at N5-H in both the photolyases. Similarly, the lower frequencies of the 1522 cm⁻¹ band in (6-4) photolyase and 1529 cm⁻¹ band in CPD photolyase, which are presumably assigned to the modes of ν_{73} - ν_{71} with N5-H bending in ν_{72}

and ν_{71} , also indicate a strong hydrogen bond at N5-H. This band was empirically used as an indicator of a hydrogen bond at N5-H in the Raman study on P-450 reductase,³² and it is justified by this study. Furthermore, judging from the lower frequencies of 1606 and 1522 cm⁻¹ in (6-4) photolyase, the N5-H hydrogen bond would be much stronger in (6-4) photolyase than that in CPD photolyase.

As mentioned above, band II of the oxidized (6-4) photolyase indicates a strong hydrogen bond at N1. This hydrogen bond would be caused by the U-shaped FAD conformation as shown in Figure 6. The proteins in this family are believed to be characterized as the unique U-shaped FAD in which an adenine ring approaches the isoalloxazine ring near the N10-C10a moiety, whose stretching significantly contributes to the ν_{61} mode of the semiquinoid form (Table 2). Therefore, the ring stacking geometry may affect the ν_{61} Raman frequency and intensity and may cause the appearance of a weak sideband at 1391 cm⁻¹ in Figure 3A. The coupled bands around 1338 cm⁻¹, which involve N3-H and N5-H bending, have a different frequency (1325 cm⁻¹) and profile from that in CPD photolyase which may indicate different H-bonding environments between these two enzymes. On all accounts, the hydrogen bonds predicted for (6-4) photolyase are similar to those of CPD photolyase and cryptochrome except a stronger interaction at N5-H, indicating a similar H-bonding environment of the flavin moiety in the DNA photolyases and blue light photoreceptor family.

Hydrophobic Environment of FAD in (6-4) Photolyase.

Resonance Raman and UV-vis absorption spectra of the oxidized FAD in (6-4) photolyase are similar to those of the isolated flavin in a nonpolar solvent. Furthermore, Raman marker bands of "buried" flavin are also observed for (6-4) photolyase. This evidence indicates that the FAD cofactor in (6-4) photolyase is placed in a hydrophobic and less polar environment, as identified for CPD photolyase.^{51,52} Spiro's model of flavin, supported by resonance Raman⁴⁶ and NMR⁵³ investigations, argued that the isoalloxazine ring prefers a zwitterionic resonance form in a polar solvent, which results in a higher frequency of band I for the oxidized flavin.³⁴ According to this model, the observed lower frequency of band I for (6-4) photolyase means a decreased polarity in a flavin pocket.

The hydrophobic environment around FAD of (6-4) photolyase was also suggested by the insensitivity of N5-H to the H/D exchange. To exchange the labile proton with solvent, water molecules must access to the exchange site. The strong hydrophobic environment in the active site of photolyase limits the approach of solvent water to N5 of the flavin ring, which also leads to difficulty in the exchange of N5-H. This coincides with the unexpected finding that N5-H deuteration proceeds little for CPD photolyase as well as (6-4) photolyase.

Low Electron Density of Ring I of FAD in (6-4) Photolyase. Previous work has shown that the C8-Cl substitution of a riboflavin binding protein exhibits a downshift of band I of the oxidized flavin ring I mode from 1631 to 1624 cm⁻¹ and weakened it greatly.⁵⁴ It is believed that the C8-Cl substitution reduces the electron density of ring I due to the electron withdrawing effect of chloride. Therefore, a significantly low-frequency and weak Raman intensity of band I (1621 cm⁻¹) observed for the oxidized (6-4) photolyase (Figure 4A) suggests that ring I of the oxidized FAD lacks electrons.

The prominent band at 1398 cm⁻¹ of FADH^o in (6-4) photolyase has a higher frequency than those of other flavins and flavoproteins. This is assignable to ν_{61} , which is an out-of-phase mode of the N1=C10-C4a-N5 stretching and ac-

cordingly sensitive to the radical character (Table 2, Figure 5). This assignment is consistent with the intensity loss of the corresponding 1391 cm^{-1} band in CPD photolyase reconstituted with $1,3,5,10\text{-}^{15}\text{N}$ -FAD.²⁸ Thus, its high frequency of 1398 cm^{-1} for (6–4) photolyase and $1391\text{--}1392\text{ cm}^{-1}$ for CPD photolyase may mean the higher radical density in the $\text{N1}=\text{C10a}-\text{C4a}-\text{N5}$ moiety. This is consistent with theoretical and EPR studies, which pointed out that FADH^\bullet has a more localized radical spin density in CPD photolyase than in other flavoproteins and a very low electron density on ring I.^{52,55} This trend is slightly stronger in (6–4) photolyase than in CPD photolyase.

One of the controlling factors of the electron density of flavin is an electrostatic effect.¹⁶ In this family of proteins, two aspartic acids (Asp372 and Asp374, numbering in *E. coli* CPD photolyase) near ring III are conserved. These negatively charged groups would readily induce an electronic perturbation to the ring system, especially to suppress the negative charge of ring III in the resonance form. Thus, the electrostatic effect from the Asp residues may contribute to keep the flavin in photolyases in the neutral form and to make an electron density of ring I low.

Biological Implication. H-bonding environment is an important factor to control the redox states of flavin in flavoproteins.¹⁶ In the study on the control of redox potentials in flavodoxin from Ludwig et al., the G57T mutant, whose hydrogen bond at $\text{N5}-\text{H}$ of flavin is expected to be weaker evaluated by crystal structure and pK_a of $\text{N5}-\text{H}$, has a significantly increased redox potential for the semiquinone/hydroquinone couple.⁵⁶ Therefore, an increased H-bonding interaction at $\text{N5}-\text{H}$ may decrease the redox potential of semiquinoid flavin and make its reduction less favorable. In photolyases, FADH^\bullet is generated during repair and must be reduced to FADH^- before the next catalytic cycle. As for CPD photolyase, the FADH^\bullet was believed to be reduced by an electron from the repaired DNA, because the quantum yield of this enzyme is almost 1.⁴ In our study, (6–4) photolyase has a similar protein environment of FAD cofactor compared with that of CPD photolyase except for a stronger hydrogen bond at $\text{N5}-\text{H}$. Therefore, this stronger hydrogen bond may decrease the redox potential of FADH^\bullet and make its reduction reaction before the next repair cycle difficult. If the FADH^\bullet in (6–4) photolyase is not reduced by repaired DNA but reduced by photoreduction from another photon, the significantly low quantum yield for this enzyme compared with CPD photolyase can be explained.

The hydrophobic and less polar environment, with small reorganization energy, will slow the back electron transfer from substrate radical to neutral semiquinoid FAD before repairing and therefore would be advantageous to electron transfer in the repairing process as pointed out for CPD photolyase.^{52,57} Such a scheme will also satisfy the repairing process of (6–4) photolyase, in which a hydrophobic environment of FAD cofactor was revealed.

Although the crystal structures of CPD photolyase showed that ring I is in the direction of the DNA lesion,^{5–8} the low spin density and possible low whole electron density on ring I implies that electron transfer between the isoalloxazine ring and CPD would not be direct.^{15,55} It was assumed that the adenine of the U-shaped FAD bridges the gap and provides effective coupling between isoalloxazine and damaged DNA.^{58,59} On the other hand, the recent study with femtosecond absorption spectroscopy concluded a direct electron jump from the FAD to the CPD, because the intramolecular electron transfer could

not be observed without substrate.⁶⁰ In (6–4) photolyase, however, a FAD cofactor with more localized spin density and moderately low electron density of ring I was observed, suggesting a higher possibility of an indirect electron transfer.

Conclusions

The resonance Raman spectra of neutral semiquinoid and oxidized forms of (6–4) photolyase were reported and interpreted with DFT calculations for the first time. The DFT calculations gave a theoretical basis for the behavior of some maker bands in relation with the environment around FAD. It is demonstrated that $\text{N5}-\text{H}$ of the FAD cofactor of (6–4) photolyase is in a hydrophobic interior and has strong H-bonding interactions with the protein, which explains its peculiar behavior in the H/D exchange as well as the low quantum yield. The unique character of Raman spectra of the oxidized form can also be interpreted in terms of electrostatic and H-bonding interactions of FAD with protein residues conserved in this family of proteins. Implications from this study will be also helpful to understand a mechanism of blue light sensor proteins such as cryptochrome 1.

Acknowledgment. This work was supported by Grants-in-Aid from the Ministry of Education, Culture, Sports, Science and Technology of Japan (MEXT) to T.K. (14001004). J.L. was supported by the scholarship from MEXT. We would like to thank Ms. Hiroko Mizuki for construction of expression vector.

Supporting Information Available: Cartesian coordinates of all calculated models. This material is available free of charge via the Internet at <http://pubs.acs.org>.

References and Notes

- (1) Lindahl, T. *Nature (London)* **1993**, *362*, 709–715.
- (2) Sancar, A. *Biochemistry* **1994**, *33*, 2–9.
- (3) Todo, T.; Takemori, H.; Ryo, H.; Ihara, M.; Matsunaga, T.; Nikaido, O.; Sato, K.; Nomura, T. *Nature (London)* **1993**, *361*, 371–374.
- (4) Sancar, A. *Chem. Rev.* **2003**, *103*, 2203–2237.
- (5) Park, H. W.; Kim, S. T.; Sancar, A.; Deisenhofer, J. *Science* **1995**, *268*, 1866–1872.
- (6) Tamada, T.; Kitadokoro, K.; Higuchi, Y.; Inaka, K.; Yasui, A.; de Ruiter, P. E.; Eker, A. P.; Miki, K. *Nat. Struct. Biol.* **1997**, *4*, 887–891.
- (7) Komori, H.; Masui, R.; Kuramitsu, S.; Yokoyama, S.; Shibata, T.; Inoue, Y.; Miki, K. *Proc. Natl. Acad. Sci. U.S.A.* **2001**, *98*, 13560–13565.
- (8) Mees, A.; Klar, T.; Gnau, P.; Hennecke, U.; Eker, A. P. M.; Carell, T.; Essen, L. O. *Science* **2004**, *306*, 1789–1793.
- (9) MacFarlane, A. W.; Stanley, R. J. *Biochemistry* **2003**, *42*, 8558–8568.
- (10) Todo, T. *Mutat. Res.* **1999**, *434*, 89–97.
- (11) Todo, T.; Ryo, H.; Yamamoto, K.; Toh, H.; Inui, T.; Ayaki, H.; Nomura, T.; Ikenaga, M. *Science* **1996**, *272*, 109–112.
- (12) Zhao, X.; Liu, J.; Hsu, D. S.; Zhao, S.; Taylor, J. S.; Sancar, A. *J. Biol. Chem.* **1997**, *272*, 32580–32590.
- (13) Sancar, A. *Science* **1996**, *272*, 48–49.
- (14) Kim, S. T.; Malhotra, K.; Smith, C. A.; Taylor, J. S.; Sancar, A. *J. Biol. Chem.* **1994**, *269*, 8535–8540.
- (15) Weber, S. *Biochim. Biophys. Acta* **2005**, *1707*, 1–23.
- (16) Miura, R. *Chem. Rev.* **2001**, *1*, 183–194.
- (17) Morris, M. D.; Bienstock, R. J. *Advances in Spectroscopy*; Clark, R. J. H.; Hester, R. E., Eds.; Wiley: New York, 1986; Vol. 13.
- (18) McFarland, J. T. *Biological Applications of Raman Spectroscopy*; Spiro, T. G., Ed.; Wiley: New York, 1987; Vol. 2.
- (19) Nakajima, S.; Sugiyama, M.; Iwai, S.; Hitomi, K.; Otsoshi, E.; Kim, S. T.; Jiang, C. Z.; Todo, T.; Britt, A. B.; Yamamoto, K. *Nucleic Acids Res.* **1998**, *26*, 638–644.
- (20) Todo, T.; Kim, S. T.; Hitomi, K.; Otsoshi, E.; Inui, T.; Morioka, H.; Kobayashi, H.; Ohtsuka, E.; Toh, H.; Ikenaga, M. *Nucleic Acids Res.* **1997**, *25*, 764–768.
- (21) Wang, B. Y.; Jorns, M. S. *Biochemistry* **1989**, *28*, 1148–1152.
- (22) Jorns, M. S.; Sancar, G. B.; Sancar, A. *Biochemistry* **1985**, *24*, 1856–1861.
- (23) Scott, A. P.; Radom, L. *J. Phys. Chem.* **1996**, *100*, 16502–16513.

- (24) Frisch, M. J.; Trucks, G. W.; Schlegel, H. B.; Scuseria, G. E.; Robb, M. A.; Cheeseman, J. R.; Montgomery, J. A., Jr.; Vreven, T.; Kudin, K. N.; Burant, J. C.; Millam, J. M.; Iyengar, S. S.; Tomasi, J.; Barone, V.; Mennucci, B.; Cossi, M.; Scalmani, G.; Rega, N.; Petersson, G. A.; Nakatsuji, H.; Hada, M.; Ehara, M.; Toyota, K.; Fukuda, R.; Hasegawa, J.; Ishida, M.; Nakajima, T.; Honda, Y.; Kitao, O.; Nakai, H.; Klene, M.; Li, X.; Knox, J. E.; Hratchian, H. P.; Cross, J. B.; Bakken, V.; Adamo, C.; Jaramillo, J.; Gomperts, R.; Stratmann, R. E.; Yazyev, O.; Austin, A. J.; Cammi, R.; Pomelli, C.; Ochterski, J. W.; Ayala, P. Y.; Morokuma, K.; Voth, G. A.; Salvador, P.; Dannenberg, J. J.; Zakrzewski, V. G.; Dapprich, S.; Daniels, A. D.; Strain, M. C.; Farkas, O.; Malick, D. K.; Rabuck, A. D.; Raghavachari, K.; Foresman, J. B.; Ortiz, J. V.; Cui, Q.; Baboul, A. G.; Clifford, S.; Cioslowski, J.; Stefanov, B. B.; Liu, G.; Liashenko, A.; Piskorz, P.; Komaromi, I.; Martin, R. L.; Fox, D. J.; Keith, T.; Al-Laham, M. A.; Peng, C. Y.; Nanayakkara, A.; Challacombe, M.; Gill, P. M. W.; Johnson, B.; Chen, W.; Wong, M. W.; Gonzalez, C.; Pople, J. A. *Gaussian 03*, revision C.02; Gaussian, Inc.: Wallingford, CT, 2004.
- (25) Franklin, W. A.; Lo, K. M.; Haseltine, W. A. *J. Biol. Chem.* **1982**, 257, 13535–13543.
- (26) Kotaki, A.; Naoi, M.; Yagi, K. *J. Biochem.* **1970**, 68, 287–292.
- (27) Su, Y.; Tripathi, G. N. R. *J. Am. Chem. Soc.* **1994**, 116, 4405–4407.
- (28) Murgida, D. H.; Schleicher, E.; Bacher, A.; Richter, G.; Hildebrandt, P. *J. Raman Spectrosc.* **2001**, 32, 551–556.
- (29) Schelvis, J. P. M.; Ramsey, M.; Sokolova, O.; Tavares, C.; Cecala, C.; Connell, K.; Wagner, S.; Gindt, Y. M. *J. Phys. Chem. B* **2003**, 107, 12352–12362.
- (30) Nishina, Y.; Shiga, K.; Horiike, K.; Tojo, H.; Kasai, S.; Matsui, K.; Watari, H.; Yamano, T. *J. Biochem.* **1980**, 88, 411–416.
- (31) Kitagawa, T.; Sakamoto, H.; Sugiyama, T.; Yamano, T. *J. Biol. Chem.* **1982**, 257, 2075–2080.
- (32) Sugiyama, T.; Nisimoto, Y.; Mason, H. S.; Loehr, T. M. *Biochemistry* **1985**, 24, 3012–3019.
- (33) Zheng, Y. G.; Dong, J.; Palfey, B. A.; Carey, P. R. *Biochemistry* **1999**, 38, 16727–16732.
- (34) Bowman, W. D.; Spiro, T. G. *Biochemistry* **1981**, 20, 3313–3318.
- (35) Abe, M.; Kyogoku, Y. *Spectrochim. Acta, Part A* **1987**, 43, 1027–1037.
- (36) Lively, C. R.; McFarland, J. T. *J. Phys. Chem.* **1990**, 94, 3980–3994.
- (37) Dutta, P. K.; Nestor, J. R.; Spiro, T. G. *Proc. Natl. Acad. Sci. U.S.A.* **1977**, 74, 4146–4149.
- (38) Kitagawa, T.; Nishina, Y.; Kyogoku, Y.; Yamano, T.; Ohishi, N.; Takaisuzuki, A.; Yagi, K. *Biochemistry* **1979**, 18, 1804–1808.
- (39) Kitagawa, T.; Fukumori, Y.; Yamanaka, T. *Biochemistry* **1980**, 19, 5721–5729.
- (40) Schmidt, J.; Coudron, P.; Thompson, A. W.; Watters, K. L.; McFarland, J. T. *Biochemistry* **1983**, 22, 76–84.
- (41) Visser, A. J. W. G.; Vervoort, J.; Okane, D. J.; Lee, J.; Carreira, L. A. *Eur. J. Biochem.* **1983**, 131, 639–645.
- (42) Bienstock, R. J.; Schopfer, L. M.; Morris, M. D. *J. Raman Spectrosc.* **1987**, 18, 241–245.
- (43) Desbois, A.; Tegoni, M.; Gervais, M.; Lutz, M. *Biochemistry* **1989**, 28, 8011–8022.
- (44) Tegoni, M.; Gervais, M.; Desbois, A. *Biochemistry* **1997**, 36, 8932–8946.
- (45) Picaud, T.; Desbois, A. *J. Biol. Chem.* **2002**, 277, 31715–31721.
- (46) Muller, F.; Vervoort, J.; Lee, J.; Horowitz, M.; Carreira, L. A. *J. Raman Spectrosc.* **1983**, 14, 106–117.
- (47) Flukiger, P.; Luthi, H. P.; Portmann, S.; Weber, J. *MOLEKEL 4.0*; Swiss Center for Scientific Computing: Manno, Switzerland, 2000.
- (48) Dutta, P. K.; Spiro, T. G. *Biochemistry* **1980**, 19, 1590–1593.
- (49) Sakai, M.; Takahashi, H. *J. Mol. Struct.* **1996**, 379, 9–18.
- (50) Brautigam, C. A.; Smith, B. S.; Ma, Z. Q.; Palnitkar, M.; Tomchick, D. R.; Machius, M.; Deisenhofer, J. *Proc. Natl. Acad. Sci. U.S.A.* **2004**, 101, 12142–12147.
- (51) Payne, G.; Wills, M.; Walsh, C.; Sancar, A. *Biochemistry* **1990**, 29, 5706–5711.
- (52) Weber, S.; Mobius, K.; Richter, G.; Kay, C. W. M. *J. Am. Chem. Soc.* **2001**, 123, 3790–3798.
- (53) Vanschagen, C. G.; Muller, F. *Eur. J. Biochem.* **1981**, 120, 33–39.
- (54) Nishina, Y.; Shiga, K.; Horiike, K.; Tojo, H.; Kasai, S.; Yanase, K.; Matsui, K.; Watari, H.; Yamano, T. *J. Biochem.* **1980**, 88, 403–409.
- (55) Kay, C. W. M.; Feicht, R.; Schulz, K.; Sadewater, P.; Sancar, A.; Bacher, A.; Mobius, K.; Richter, G.; Weber, S. *Biochemistry* **1999**, 38, 16740–16748.
- (56) Ludwig, M. L.; Patridge, K. A.; Metzger, A. L.; Dixon, M. M.; Eren, M.; Feng, Y. C.; Swenson, R. P. *Biochemistry* **1997**, 36, 1259–1280.
- (57) Heelis, P. F.; Hartman, R. F.; Rose, S. D. *Chem. Soc. Rev.* **1995**, 24, 289–297.
- (58) Antony, J.; Medvedev, D. M.; Stuchebrukhov, A. A. *J. Am. Chem. Soc.* **2000**, 122, 1057–1065.
- (59) Medvedev, D.; Stuchebrukhov, A. A. *J. Theor. Biol.* **2001**, 210, 237–248.
- (60) Kao, Y. T.; Saxena, C.; Wang, L. J.; Sancar, A.; Zhong, D. P. *Proc. Natl. Acad. Sci. U.S.A.* **2005**, 102, 16128–16132.